On localisation with robust power control for safety critical wireless sensor networks.

Michael J. Walsh [1], Anthony Fee [2], John Barton [1], Brendan O'Flynn [1], Martin J. Hayes [2], Cian O'Mathuna [1],

(1Clarity Center for Web Technologies, Microsystems Centre - Tyndall National Institute Lee Maltings, University College Cork, Ireland)

(2Wireless Access Research Center, University of Limerick, Limerick, Ireland)

Abstract: A hybrid methodology is proposed for use in low power, safety critical wireless sensor network applications, where quality of service orientated transceiver output power control is required to operate in parallel with radio frequency based localisation. The practical implementation is framed in an experimental procedure designed to track a moving agent in a realistic indoor environment. An adaptive time synchronised approach is employed to ensure the positioning technique can operate effectively in the presence of dataloss and where the transmitter output power of the mobile agent is varying due to power control. A deterministic multilateration based positioning approach is adopted and accuracy is improved by filtering signal strength measurements overtime to account for multipath fading. The location estimate is arrived at by employing least square estimation. Power control is implemented at two separate levels in the network topology. Firstly power control is applied to the uplink between the tracking reference nodes and the centralized access point. A number of algorithms are implemented highlighting the advantage associated with using additional feedback bandwidth, where available, and also the need for effective time delay compensation. The second layer of power control is implemented on the uplink between the mobile agent and the access point and here quantifiable improvements in quality of service and energy efficiency are observed. The hybrid paradigm is extensively tested experimentally on a fully compliant 802.15.4 testbed, where mobility is considered in the problem formulation using a team of fully autonomous robots.

Keywords: Wireless Sensor Network; Power Control; Localisation

1 Introduction

Wireless ambient intelligent technology will soon emerge from the research laboratories around the world and become embedded in everyday life. Among the challenges that remain before this technology becomes truly pervasive is that of positioning, both for the wireless device and perhaps more importantly for the event that occurs within proximity of the device. Many applications by their very nature require a means of localizing the devices that comprise the network. This information can be used in a variety of ways ranging from simply locating the closest printer to positioning a rescue worker or injured party in a disaster scenario.

Wireless sensor networks (WSNs) have begun to play a central role in the integration of this ubiquitous computing. Among the distinguishing features of WSN technology is its seamless interaction with the surrounding environment achieved through pervasive sensing and wireless communication. This in turn provides a great deal of flexibility and WSNs are now envisaged as a viable tool in safety critical applications such as search and rescue where the wired alternative can be logistically impossible or indeed damaged during the event itself [1, 2].

As these networks are expected to operate for periods of years without battery replacement it is unsurprising that more computationally intensive and power hungry localisation technologies such as the global positioning system (GPS) [3] will be used sparingly. This requirement is coupled with the fact that these location based networks must operate in indoor environments as well as in outdoor areas of dense settlement and infrastructure where a GPS signal may not be available. Not surprisingly to overcome these shortcomings alternative low power and computationally efficient localisation techniques have been proposed (see [4] and references therein).

However accurate positioning information is not the only concern that must be addressed before safety critical WSN solutions become truly useful. Communications reliability or quality of service (QoS) is also of key concern. To highlight this it is worthwhile considering a recent deployment [5], where wireless controlled robotic instruments equipped with sensors, were sent into dangerous environments to access the possible danger to human rescue teams, who were to enter the environment once deemed safe. Following completion of the initial test phase, empirical observation showed that more then two-thirds of the wireless systems had lost connection with their operators. This result was influenced heavily by the phenomenon known as the near-far effect, which occurs when one user operating at a much higher output power then another drowns out the weaker signal. Transceiver output power control is an effective means of combating the near-far effect as well as other factors impinging on QoS such as channel attenuation and interference. Transceiver output power control is by no means a new topic and much progress in the area has been reported in recent times [6∼9].

1.1 Combining RF based Localisation with Transceiver Output Power Control

Clearly both localisation and power control have received significant attention as separate research strands. However consider the case when both location specific informa-

Tyndall is a part of the CLARITY CSET supported by Science Foundation Ireland under grant 07/CE/I1147".

tion and highly reliable communications are prerequisite. A problem immediately arises as many localisation strategies are reliant on measuring the radio frequency (RF) channel in some regard and power control as a matter of necessity augments said entity. For example many localisation methodologies measure signal strength at a number of spatiotemporal points and use this information as a means of estimating position. Power control on the other hand varies transceiver output power which directly affects signal strength. The result can be inaccurate positioning due to a rapidly varying RF channel. Couple this with dataloss due to collisions and asynchronous communication links and this inevitably makes a combined solution far more difficult to realize. An effective hybrid localisation power control implementation must therefore be robust to information loss and to channel fluctuations which occur as a result of a constantly changing transmitter power as well as from channel attenuation and interference.

With this in mind, work presented here is focused on the joint task of providing accurate localisation and QoS based power control over a realistic WSN scenario. A systems theoretic solution is proposed and is presented here in three parts. Firstly an RF based deterministic localisation algorithm is outlined that combines a number of existing strategies into a hybrid multilateration technique using least square estimation (LSE). Secondly a number of power control algorithms are introduced to alleviate the near-far effect and to limit the negative impact of attenuation, interference and noise. Finally an adaptive time synchronised approach is employed to ensure the positioning technique can operate effectively despite a varying transmitter output power from the mobile agent due to power control. To practically test the proposed hybrid methodology, an extensive fully scalable and repeatable experimental testbed has been developed. The testbed is highly effective from a repeatability and performance perspective and consists of a number of 802.15.4 compliant wireless embedded platforms, autonomous robot agents used to introduce mobility and emulate human movement, and a scaled model of a building to establish realistic fading conditions.

2 A Methodology for Hybrid Localisation Power Control

2.1 RF Localization for Wireless Sensor Networks

Localization methods using RF signals are categorised as being either *range based* or *range free*. Range based methods exploit information about the distance between neighboring nodes. Although the distance cannot be measured directly it can, theoretically, be derived using delay measurements taken on data travelling between nodes or from analysis of the signal attenuation. There are many examples in the literature of this approach to localization (see [10∼12] and references therein). A range based approach tends to impose quite severe constraints on any given scenario and therefore one particular scheme can outperform another in a rather arbitrary fashion based on the node or beacon deployment density that is outside the control of the engineer. Couple this with the need to establish a well defined mathematical or empirical model relating signal attenuation or delay to exact distance and the resulting scheme can be overly conservative. In fact recent empirical evidence suggests that assumptions based on estimating distance from signal attenuation measurements do not hold up well in practice [13]

On the other hand, range free localization estimates the position of an unknown node using other means. For example in [14] a range free localization technique is employed where the Received Signal Strength (RSS) value at an unknown node is compared with RSS values for its neighbours and based on this comparison a decision is made whether the unknown node location is inside geometric triangles formed by reference nodes or nodes whose position is known. Clearly range free methods offer added flexibility, given no direct correlation between RSS and distance need be established. A range free approach similar to this is adopted here and there follows a description of the methodology used to estimate location based on filtered RSS data observed at a number of reference nodes.

2.1.1 Range Free Deterministic Localisation

As mentioned previously, to avoid an overly conservative design methodology a weak assumption is made by stating that as a node moves away from a reference node, the RSS observed at that reference node, when appropriately filtered to remove multipath effects, will decrease as the node travels further from the reference node. Then assuming there are a number of reference nodes within transmission range of the mobile node a positioning decision based on all available filtered RSS data can be made. Filtering the RSS removes multipath effects and can as a result lead to more accurate localisation especially when tracking a mobile object. Fig 1 illustrates how filtering can extract the more useful information from an RSS signal.

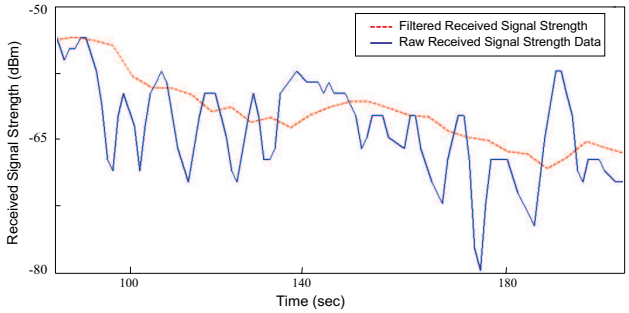

Fig. 1 Received Signal Strength (RSS) filtered to remove multipath effects.

Initial data processing for the proposed methodology is carried out by employing a variant of a class of localization strategies known as Ecolocation [15]. It's ease of implementation and improved performance when compared with other more computationally intensive algorithms offers an ideal solution to the problem at hand.

The technique is adapted for use in a situation where a mobile node MN, whose position is to be estimated, exhibits a variable output power as a result of dynamic power management. MN is localised by firstly calculating the distance between each grid point (i, j) in the localization area, and each reference node RN_k whose positions are assumed known and are represented by $(x_{RN_k},\ y_{RN_k})$. This distance is calculated from

$$d_{RN_k} = \sqrt{(x_{RN_k} - i)^2 + (y_{RN_k} - j)^2} \qquad (1)$$

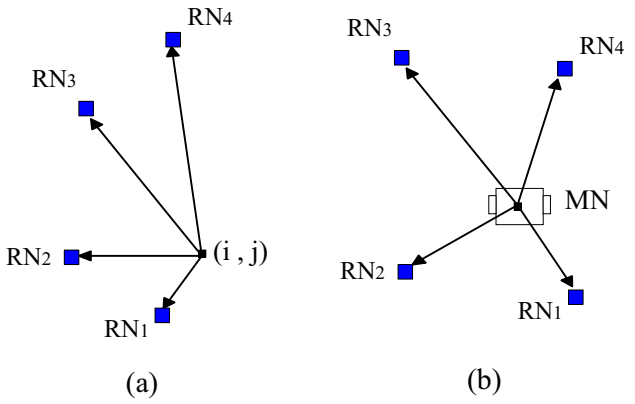

Fig. 2 The reference nodes RN_i are ordered dependant on distance in descending order. In (a) for instance this would be (RN_4 RN_3 RN_2 RN_1)

These values are subsequently stored in a matrix D^{ij}. The distances for each grid point (i, j) are arranged in descending order and their respective reference node numbers are then stored. Hence for the simple scenario in Fig. 2, the values [4 3 2 1] are stored in R^{ij}. Experimental real-time RSS measurements, taken at MN are then arranged in descending order and their reference node numbers recorded and denoted by the vector $\overrightarrow{mn}$. Again, for the simple scenario in Fig. 1(b) the vector $\overrightarrow{mn} = [3\ 2\ 4\ 1]$. An iterative algorithm then compares each element in R^{ij} to the sorted reference node vector $\overrightarrow{mn}$ and any match(es) is(are) recorded.

The recorded match is then used to calculate the estimated position of MN. To achieve this, position is determined based on a Least Square Estimate (LSE), [16]. Assuming the position of each reference node $RN_k,\ k \in 1..L$ is known to be $(x_{RN_k},\ y_{RN_k})$ and the distance to each node from the estimated position of MN is d_{RN_k}, then for any two reference nodes RN_i and RN_j the section boundaries can be computed to be:

$$d_{RN_i}^2 - d_{RN_j}^2 = (x_{MN} - x_{RN_i})^2 + (y_{MN} - y_{RN_i})^2$$

$$-(x_{MN} - x_{RN_j})^2 - (y_{MN} - y_{RN_j})^2 \qquad (2)$$

where $p_{MN} = (x_{MN},\ y_{MN})^T$ is the estimated position of MN. p_{MN} can be calculated from:

$$H.p_{MN} = C \qquad (3)$$

with

$$H = \begin{bmatrix} h_{x(2,1)} & h_{y(2,1)} \\ \vdots & \vdots \\ h_{x(L,1)} & h_{y(L,1)} \\ \vdots & \vdots \\ h_{x(L,L-1)} & h_{y(L,L-1)} \end{bmatrix},\ p_{MN} = \begin{bmatrix} x_{MN} \\ y_{MN} \end{bmatrix}$$

$$C = \begin{bmatrix} c_{2,1} \\ \vdots \\ c_{L,1} \\ \vdots \\ c_{L,L-1} \end{bmatrix} \qquad (4)$$

where

$$h_{x_{RN}}(i,j) = 2(x_{RN_j} - x_{RN_i})$$
$$h_{y_{RN}}(i,j) = 2(y_{RN_j} - y_{RN_i})$$

and

$$c_{i,j} = d_{RN_i}^2 - d_{RN_j}^2 + x_{RN_j}^2 - x_{RN_i}^2 - y_{RN_j}^2 - y_{RN_i}^2$$

The location estimation is then determined from:

$$p_{MN}^T = (H^T H)^{-1} H^T C \qquad (5)$$

2.2 Wireless Sensor Network Power Control

2.2.1 The System Model

To provide some intuitive understanding for the modelling work that has been carried out, consider the following simplified scenario consisting of two access points and two mobile nodes. Note that, throughout, a value in the linear scale is represented by $\bar{g}$ and g is it's corresponding value in dB namely $g = 10log_{10}\bar{g}$, where $\bar{g}(k)$ is a time-varying multiplicative power gain. From Fig. 3, MN_1 and MN_2 are connected to AP_1 and AP_2 respectively and therefore the signals $\bar{g}_{11}$ and $\bar{g}_{22}$ are the the required for communication. However the signals $\bar{g}_{12}$ and $\bar{g}_{21}$ are generated interference. The downlink (BS to MN) only is considered here for simplicity. The gains/attenuations for this simple network in its entirety can be arranged in a gain matrix:

$$G = \begin{pmatrix} \bar{g}_{11}\ \bar{g}_{12} \\ \bar{g}_{21}\ \bar{g}_{22} \end{pmatrix}$$

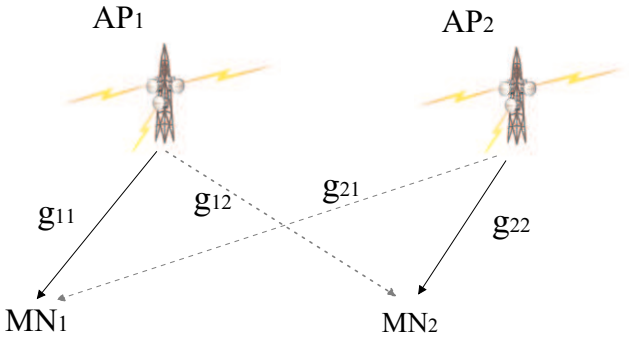

Fig. 3 Simple communication scenario with direct signals (solid lines) and interference (dashed lines)

The transmitted power from a access point AP_i at time instant k is given by $\bar{p}_i(k)$. From Fig. 3 MN_1 receives signal power $\bar{p}_1(k)\bar{g}_{11}(k)$ and interference power $\bar{I}_1(k)$ denoted:

$$\bar{I}_1(k) = \bar{q}_2(k)\bar{p}_2(k)\bar{g}_{12}(k) + \bar{n}_1(k) \qquad (6)$$

where $\bar{n}_1$ denotes the noise power and $\bar{q}(k)$ is a binary random variable modelling transmission attempts of the nodes.

Therefore if MS_2 is transmitting it has $\bar{q}_2(k) = 1$ and $\bar{q}_2(k) = 0$ otherwise. Note that the probability $P_r(\bar{q}_2(k) = 1) = \alpha_i$ and accordingly the probability $P_r(\bar{q}_2(k) = 0) = 1 - \alpha_i$. The SINR at MS_1 can thus be represented by:

$$\bar{\gamma}_1(k) = \frac{\bar{p}_1(k)\bar{g}_{11}(k)}{\bar{I}_1(k)} = \frac{\bar{p}_1(k)\bar{g}_{11}(k)}{\bar{q}_2(k)\bar{p}_2(k)\bar{g}_{12}(k) + \bar{n}_1(k)} \quad (7)$$

In dB the SINR can be represented by:

$$\gamma_1(k) = p_1(k) + g_{11}(k) - I_1(k) \quad (8)$$

It is worth noting in this instance that if $\bar{q}_2(k) = 0$ the system is said to be noise limited and that the channel qualitative measure reverts to Signal to Noise (SNR) ratio. Following this the SINR of the i-th node for a network consisting of n nodes communicating with an access point is given by:

$$\bar{\gamma}_i(k) = \frac{\bar{p}_i(k)\bar{g}_i(k)}{\sum\limits_{j\in\mathcal{Z}, i\neq j} \bar{q}_j(k)\bar{p}_j(k)\bar{g}_j(k) + \bar{n}_i(k)} \quad (9)$$

where $\bar{n}_i$ is the power of the white noise at the access point to which the i-th is communicating. $\sum\limits_{j\in\mathcal{Z}, i\neq j} \bar{q}_j(k)\bar{p}_j(k)\bar{g}_j(k)$ is the sum of the interference from all nodes simultaneously communicating with the access point and $\mathcal{Z}$ is the set of all nodes interfering with node i. Representing (8) in dB results in:

$$\gamma_i(k) = p_i(k) + g_i(k) - I_i(k) \quad (10)$$

Using statistical models $g_i(k)$ can be represented by:

$$g_i(k) = l_i(k) + s_i(k) + m_i(k) \quad (11)$$

where the distance dependent attenuation and the antenna attenuation are modelled by the path loss $l_i(k)$. Terrain variation resulting in shielding and diffraction is modelled by the shadow fading $s_i(k)$, while multipath fading $m_i(k)$ captures the effects of reflection. The following equations represent these uncertain factors [18]:

$$l_i(k) = l_o - 10\eta log_{10}(x_i), \quad (12)$$

$$s_i(k) = \xi(k)10log_{10}e \quad (13)$$

$$m_i(k) = X^2. \quad (14)$$

where l_o is the path loss computed at a reference distance. Here, the reference distance is assumed to be zero and hence l_o is also assigned the value zero. The distance between the access point and the i-th node is given by x_i. The path loss exponent is represented by η whose value is normally in the range of 2 to 4 (where 2 is for propagation in free space, 4 is for relatively lossy environments and for the case of full specular reflection from the earth surface, the so-called flat-earth model). ξ is a Gaussian random variable with zero average and standard deviation σ_ξ. X is a random variable whose distribution is Gaussian if a clear LOS is available and both the transmitter and receiver are in situ. If a clear LOS is present and one or both of the endpoints are moving the variable will have Ricean distribution and if no LOS component is present and either of the endpoints are moving the variable will have Rayleigh distribution.

Calculating Bit Error Rate from RSS: A similar approach to [17] is used to directly estimated the SINR and subsequently bit error rate (BER) using the RSS. A setpoint or reference RSSI value can thusly be selected and related directly to packet error rate (PER) as outlined in the 802.15.4 standard [19]. To expand, the BER for the 802.15.4 standard operating at a frequency of 2.4GHz is given by:

$$BER = \frac{8}{15} \times \frac{1}{16} \times \sum_{k=2}^{16} -1^k \binom{16}{k} e^{20\times SINR\times(\frac{1}{k}-1)}, \quad (15)$$

and given the average packet length for this standard is 22 bytes, the PER can be obtained from:

$$PER = 1 - (1 - BER)^{PL} \quad (16)$$

where PL is packet length including the header and payload. Establishing a relationship between RSS and SINR and subsequently PER can therefore help to pre-specify levels of system performance. From [17] the SINR is given by:

$$10log_{10}\bar{\gamma}_i(k) \approx RSSI_i(k) - n_i(k) - C - 30 \quad (17)$$

where the addition of the scalar term 30 accounts for the conversion from dBm to dB and C is the measurement offset assumed to be 45 dB from [19]. The SINR in dB is thus:

$$\gamma_i(k) = 10^{(RSSI_I(k) - n_i(k) - C - 30)/10}. \quad (18)$$

2.2.2 Log Linear Power Control Algorithms

Consider the arrangement of Fig. 4. The performance objective here is to measure the actual SINR $\gamma(k)$ and to compare it with a prescribed attainable target SINR value $\gamma_t(k)$. This target value is directly relatable to RSS using equation (17). The controller outputs a value which in essence determines whether the mobile user increases or decreases its transmission power. A similar approach to [20] is adopted here with $G_i(q) = \frac{\beta}{q-1}$ representing the case where:

$$p_i(k+1) = p_i(k) + \beta e_i(k) \quad (19)$$

which is an integrating controller with $C_i\{e_i(k)\} = e_i(k)$.

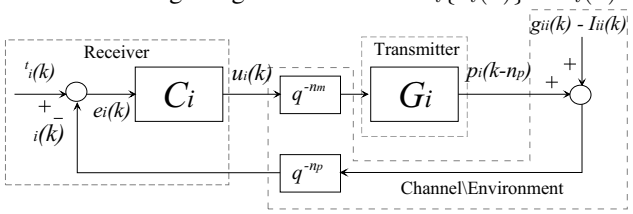

Fig. 4 Block diagram of the receiver-transmitter pair *i* when employing an SIR-based power controller

Assuming:

$$C(q) = \frac{\beta}{q-1},\ u_i = p_i,\ G_i\{p_i(k-n_p)\} = p_i(k-n_p) \quad (20)$$

is a more natural interpretation allowing for a number of different designs to be implemented as C_i where q is the forward shift operator [20]. There are two important feedback classes that should be considered when implementing radio power control. The first is *information feedback*, as in (19) above, where exact measurements are fed back from the transmitter. In this instance the error is:

$$e_i(k) = \gamma_i^t - \gamma_i(k). \tag{21}$$

A second approach is *decision feedback* where the sign of the error alone is fed back resulting in:

$$s_i(k) = sign(\gamma_i(k) - \gamma_i(k)) = sign(e_i(k)) \tag{22}$$

This method requires just one bit for signalling which is extremely bandwidth efficient. When utilizing decision feedback, as in [21], the simple Integral (I) controller in (19) takes the form:

$$p_i(k+1) = p_i(k) + \beta s_i(k) \tag{23}$$

The controller in (23) above is often referred to as a *Fixed Step* size power law where the power $p_i(k)$ is increased or decreased by β depending on the sign of the error $e_i(k)$. An *Adaptive Step* size power control uses the same power control law as a fixed step approach (23), however the parameter β is updated depending on system requirements according to the following:

$$\beta(k) = [\alpha\beta^2(k-1) + (1-\alpha)\sigma_e^2]^{\frac{1}{2}} \tag{24}$$

where as before σ_e is the sampled standard deviation of the power control tracking error and α is the forgetting factor, introduced to smooth a measured SINR signal that may be corrupted by noise. *Adaptive Step* size power control can therefore be represented as:

$$p_i(k+1) = p_i(k) + \beta(k) s_i(k) \tag{25}$$

Anti-Reset Windup: The use of an integrator (I) in the controller presents within itself a problem when addressing the system constraints. When the hardware output power limitations, represented by $[P_{min}, P_{max}]$ are surpassed, the loop is effectively open. In particular, if the control is such that a long period of saturation exists, it is possible for the integral term to keep integrating even when it is not reasonable to do so. The integrator itself is open-loop unstable, and the integrator output will drift higher(lower). This is known as integrator windup.

A simple solution lies in the use of Anti-Reset [22], where the integral output is recomputed so as to keep the control at the saturation limit. A filter is used to ensure the anti-reset is not limited by short periods of saturation that may be introduced by noise. In essence an additional feedback path is added around the integrator to stabilize the integrator when the main feedback loop is effectively open due to saturation. Thus if the integrator state is $x_i(k)$ it is updated according to:

$$x_r(k) = x_i(k) + \frac{1}{T_t}(f(p_i(k)) - p_i(k)), \tag{26}$$

where the constraints $[P_{min}, P_{max}]$ are described by the static memoryless nonlinear function $f(.)$, $x_r(k)$ is the recomputed integrator state and T_t is a tracking parameter. Note that if no saturation exists $f(p_i(k)) = p_i(k)$, $x_r(k)$ is equal to $x(k)$. In general the smaller T_t is the quicker the reset, however this rule of thumb is noise limited where if the chosen value is too small noise will prevent the integrator from resetting.

Smith Prediction: Time Delay Compensation: Variable time delay imposes a severe performance constraint on the closed loop performance of a power aware network based application. One approach to the compensation of Time delay systems, (particularly in the process industries), is through the use of a Smith predictor [22]. In essence the Smith Predictor is implemented as per the arrangement in Fig. 4 by:

$$\tilde{\gamma_i}(k) = \gamma_i(k) + p_i(k) - p_i(k - n_m - n_p) \tag{27}$$

where $\tilde{\gamma_i}(k)$ is an adjusted SINR measurement at the receiver.

2.3 Combined Localisation and Power Control

The key to combining a localisation and power control strategy is time syhchronisation. Consider the configuration in Fig. 5. The mobile node MN sends a single packet to each reference node RN_i. Each reference node in turn calculates the RSS and communicates this value to a central processing point or base station BS, where the position is determined using the methodology outlined in section 2.1. Consider the case where due to mobility or asynchronous connectivity communication fails between MN and one of the reference nodes or indeed between the base station BS and one of the reference nodes. In this instance while the localisation algorithm can still be solved using information extrapolated from previous RSS samples the accuracy will inherently be negatively impacted. Concurrently power control updates the output power of MN at a higher rate then localisation calculation to account for interference and multipath channel attenuation. This introduces additional and possibly large inaccuracies in the positioning of the mobile node.

This work proposes an adaptive time synchronised solution that accounts for dataloss and the rapidly varying output power of the mobile node due to power control. A flowchart outlining this approach is illustrated in Fig. 6. The methodology comprises of a number of steps namely:

(1) Each packet communicated by MN is time stamped and this time stamp is forwarded along with the RSS measurement recorded at each reference node RN_i to the base station BS. This ensures the RSS measured at each of the reference nodes has been transmitted by MN using an equal transceiver output power level.

(2) The base station BS then determines by examining the time stamp information if there is missing RSS information. If missing data is detected the base station instructs MN to retransmit its packet to the reference nodes which in turn will forward new time stamped RSS updates to the base station. A threshold is placed on the number of invoked retransmissions and this number is directly influenced by the tolerable latency

in the network.

(3) If the threshold number of retransmissions is reached and there still remains missing RSS data required for the positioning algorithm, the look-up table described in section X is recompiled omitting the reference nodes associated with missing or dated RSS data. In this manner old RSS data possibly associated with a different transceiver output power level is discarded.

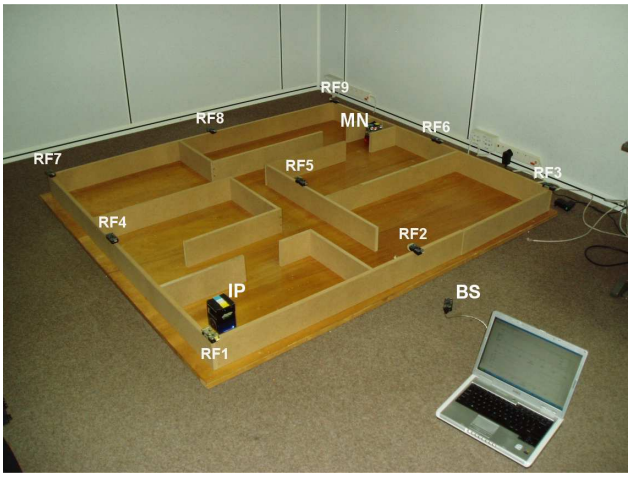

Fig. 5 Experimental scenario consisting of a scalable model of a building, nine reference nodes RF1-9, a rescue robot MN with onboard mobile node and a robot 'civilian' or injured party IP.

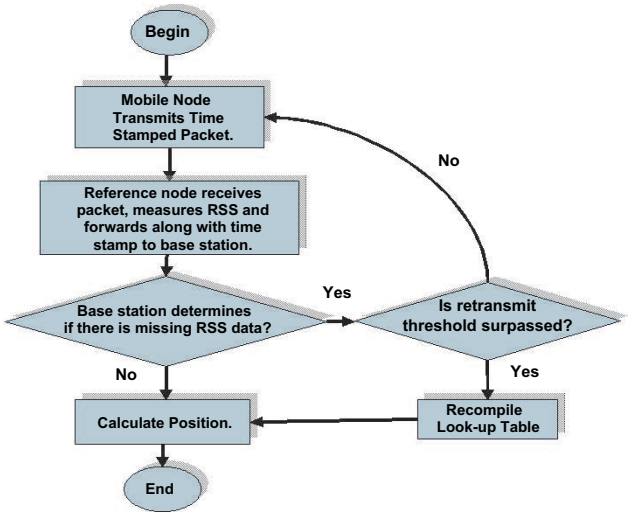

Fig. 6 Flowchart for the adaptive time synchronised solution that accounts for dataloss and the rapidly varying output power of the mobile node due to power control.

3 Practical Implementation

3.1 Search and Rescue Testbed Description

To illustrate the use of the localisation and power control algorithms in practice, an application was formulated based upon a derivation of that used in RoboRescue [23]. The objective of this scenario is to program a robot to enter a building, explore its surrounding environment, attempt to locate a second "civilian" robot, and then act as a guide to safety via a mapped exit route. Theoretically the rescuer would be in possession of a wireless 'wearable' device and would be continually informed of an exit route via this device.

As illustrated in Fig. 5, the experimental setup consists of a scaled surface measuring 2 meters squared. The testbed consists of nine fixed position reference nodes, one access point coordinator and one mobile node. The Tmote Sky mote sensor node is an embedded platform using an 802.15.4 compliant transceiver and is selected as the primary embedded platform for this work [24]. The Tmote platform employs the CC2420 transceiver using the Direct Sequence Spread Spectrum (DSSS) technique to code the required data. Carrier Sensing Multiple Access/Collision Avoidance (CSMA/CA) is then used to transmit the coded packets. The CC2420 transceiver on the Tmote platform provides an received signal strength indicator (RSSI) measurement in dBm by averaging the received signal power over 8 symbol periods or 128μs. The mobile node is attached to an autonomous robot, the MIABOT Pro fully autonomous miniature mobile robot [25]. The access point is connected directly, via usb connection, to a power control where the power aware localization algorithm is implemented in a centralised fashion. The second robot, the civilian, is randomly situated in any of the rooms within the environment.

A requirement for this experiment is that the rescue robot be equipped with sensors capable of detecting and avoiding obstacles in its proximity, thus enabling navigation of the scaled building model. The rescue robot is therefore equipped with an 8-way sonar turret for the purpose of distance measurement, as well as optical encoders on each wheel to accurately measure the distance traveled. The robots are differentially driven with motor controllers outputting separate Pulse Width Modulation (PWM) signals for each stepper motor. The robots are controlled using an Atmel ATMega64 microcontroller which runs at a speed of 14.5MIPS and is equipped with a 64kb flash. The ATMega64 is manually programmed using the GNU Compiler Collection (GCC) 'C' compiler. Commands are communicated to each robot through a Bluetooth hub.

3.2 Autonomous Robot Program

Initially the primary robot, the rescuer, would be placed at the entrance to the building as in Fig. 5. It is assumed that the rescue robot is consistently receiving localisation information accurate to within 15cm. To optimise the use of both the localisation and the robots local sensors, the environment is separated into a grid system, with each grid measuring 20cm x 20cm. The robot explores each grid section in turn. For simplicity it is assumed that each grid can only contain a maximum of one junction. A junction is defined as an area in the building where at least one entrance to a room meets the hallway. The algorithm shown in the left hand column of table 1 is executed by the rescue robot until the civilian robot is located. Once this occurs, the algorithm portrayed in the right hand column of table 1 cycles until the civilian robot has arrived at the building exit. The civilian robot is thusly escorted to safety by the rescue robot.

3.3 Localization

The localization technique was implemented as follows. The mobile node positioned on the MIABOT communicated information to each of the reference nodes. Upon receiving a packet from the mobile agent each reference node calculated the RSSI and upon reception of five packets the recorded RSSI data was sent to the base station for process-

Table 1
Pseudo code for autonomous robot programming

RESCUE ROBOT PROGRAM	CIVILIAN ROBOT PROGRAM
Rescue Robot placed at entrance to building.	Civilian Robot is located randomly within
Exit position is recorded via localization.	the building.
0 Exit position: $(x, y) \rightarrow (191, 124)$.	0 Current position: Unknown
1 **If junction encountered**	1 **If Rescue Robot enters room**
2 Record Junction Position and Branches	2 Follow Rescue Robot to building exit
3 Junct. Pos. = (x_{jun}, y_{jun}), Branches = (r, l, a)	3 **Else**
4 Explore each branch in turn	4 Stay in situ, wait for Rescue Robot
5 **If Civilian found**	
6 Escort civilian to exit via mapped escape route	
7 **Else**	
8 **If hallway not fully explored**	
9 Proceed forward continue search	
10 **Else**	
11 Return to previous junction or building exit	
12 **Else**	
13 Proceed forward continue search	

ing. The base station then performs the adaptive time synchronised solution illustrated in Fig. 6 before filtering the RSSI data to remove any multipath component which would lead to erroneous results. A low pass empirically determined filter was used in this instance taking the form:

$$F = \frac{0.25z}{z - 0.75} \tag{28}$$

The data was then arranged in descending order of magnitude and compared to the comparison matrix D^{ij} containing some 23409 elements and with a possible 2601 location matches. In this experiment D^{ij} contains samples taken at a spacing of $2cm$. The MIABOT implements the algorithm outlined in table 1 and the localization technique was engaged to record/predict position at regular 5 second intervals. The results are shown in Fig. 7 and are quite promising as the mobile node is successfully localised using the aforementioned technique. Factors that have been shown to affect these results in this scenario are the inefficiency of the filter ability to remove a multipath signal component and the effect of antenna orientation [1].

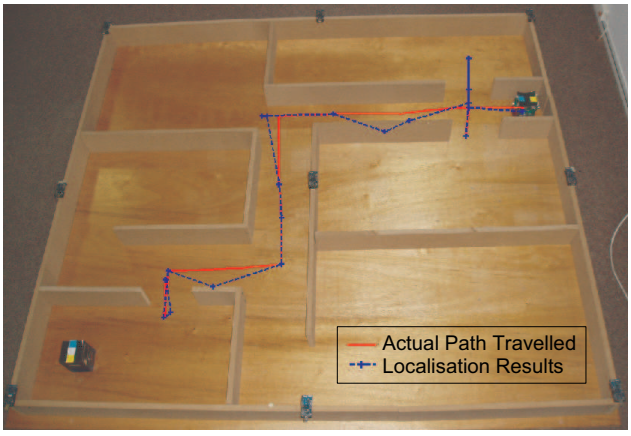

Fig. 7 Localization test results.

3.4 Power Control Observations

As the reference nodes are themselves wireless devices and are assumed to have limited available power, the performance objective at hand is to keep nodes transmitting at as low a power as possible, thereby lengthening battery lifetime. Power control in this scenario is used to compensate for interference generated by surrounding nodes and other noise that may be exogenous to the system in question. Given that the reference nodes and the base station are in situ, there is no Rayleigh fading present at the receiver and therefore power control is more straightforward. To ensure that a reliable connection is maintained between the mobile node and the base station in this context, power control is implemented on the uplink connection. Uncertain factors that are considered in this scenario are the motion of the transmitter and hence a parameterised incorporation of multipath fading within the signal observed at the receiver.

3.4.1 System Parameters and Performance Criteria

Sampling frequencies of $T_s = 1(sec)$ and $T_s = 5(sec)$ are selected for the mobile node and stationary reference nodes respectively. A target RSSI value of -55dBm is selected for the mobile node, guaranteeing a PER of $< 1\%$, verified using equations 15, 16 and 17. To optimize power consumption a setpoint of -65dBm is chosen for the reference nodes, assuming the absence of deep fading associated with mobility. The *standard deviation* of the RSSI tracking error is chosen as a performance criterion:

$$\sigma_e = \left\{ \frac{1}{S} \sum_{k=1}^{S} [RSSI_{target} - RSSI(k)]^2 \right\}^{\frac{1}{2}} \tag{29}$$

where $RSSI_{target}$ is the setpoint RSSI, -55dBm and -65dBm for the mobile and reference node case respectively, S is the total number of samples and k is the index of these samples. *Outage probability* is defined as

$$P_o(\%) = \frac{number\ of\ times\ RSSI\ <\ RSSI_{th}}{the\ total\ number\ of\ iterations} \times 100 \tag{30}$$

where $RSSI_{th}$ is selected to be -60dBm and -70dBm for the mobile and reference node case respectively. For each case any value below this is deemed unacceptable in terms of PER performance. This can be easily verified again using equations (17), (15) and (16). To fully access each paradigm, some measure of power efficiency is also useful and a detailed evaluation of each algorithms energy usage is

[1] TinyOS and Matlab code used in this experiment is available open source from the authors. Email: michael.walsh@tyndall.ie

outlined below.

3.4.2 Reference Node Power Control

Each of the power control algorithms introduced in section 4 was tested in concert with the aforementioned localization procedure. For purposes of clarity only, links three, five and seven are represented graphically in Fig. 8. Here, the results for fixed step power control represented by equation (23) are illustrated. The bottom of Fig. 8 shows the output power level (or controller actuator) value. This value is written to the CC2420 transceiver and represents the amplitude of the RF wave. Thus, the higher the value that is written to the transceiver the greater the RF wave amplitude and the more power consumed by the network. Clearly the distance from the base station directly also influences the output power level, with link 7 located furthest away, this node obviously needs to transmits at a higher power. The limiting effect of decision feedback in this context is noted at this point of the analysis.

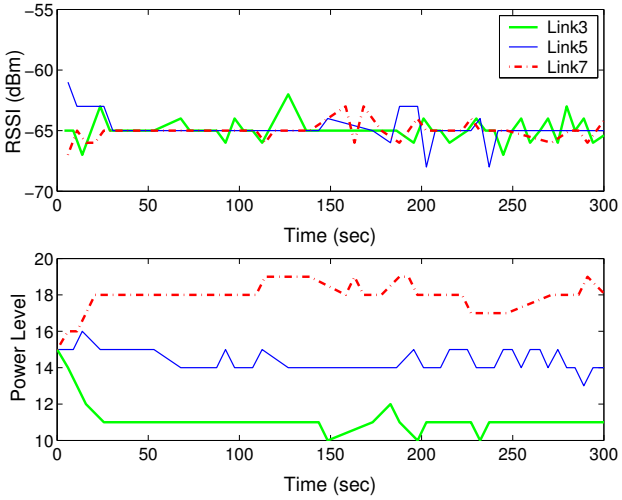

Fig. 8 Fixed Step Power Control (equation (23)) with $\beta = 1$. Where Link 3 is the thick line, Link 5 is the thin solid line and Link 7 is dashed line

Fig. 9 shows the system response for a number of other controller parameter values and configurations. Fig. 9(a) shows the fixed step size configuration with $\beta = 2$. The increased step size does not improve the system output and in fact when compared to Fig. 8 the response proves to be more oscillatory. In Fig. 9(b) the response shows improvement with a fixed step size $\beta = 1$ and Smith prediction with roundtrip delay assumed to be one. Increasing the step size to $\beta = 2$ with Smith prediction, shown in Fig. 9(c), as in the previous instance does not further improve the system performance and in fact as before a more oscillatory output is observed.

Adaptive step size power control, using equation (25) is implemented next and the response shown in Fig. 9(d) shows considerable improvement on the previous four configurations. The forgetting factor is set to 0.95 to help smooth the measured RSSI value and this explains the enhanced performance. In Fig. 9(e) information feedback is used to implement equation (19) using $\beta = 0.35$ as suggested by [26]. The added flexibility associated with the use of information feedback is very apparent here. A significant improvement in tracking performance is observed with this scheme. To compensate for the effect of roundtrip delay, which here is nominally suggested to be one sampling period, Smith prediction is added to the system. Clearly from Fig. 9(e) this configuration offers excellent nominal performance.

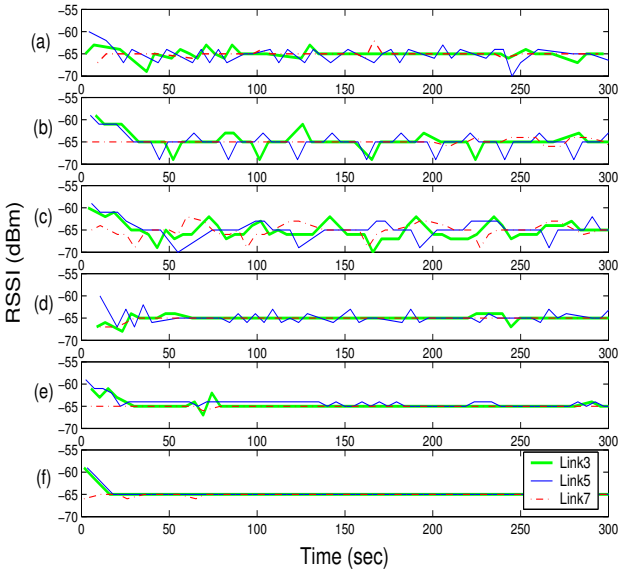

Fig. 9 Reference Node Power Control

3.4.3 Mobile Node Power Control

As stated previously the difficulty in implementing power control for a mobile node is the presence of multipath fading in the received RSSI signal. With this in mind its seems natural to rule out decision feedback based control entirely unless is is impossible to do so, i.e. when limited bandwidth is available. To demonstrate why this is advisable, the configuration shown to perform best for the reference node power control using decision feedback was implemented on the uplink between the mobile node and the base station. The results are shown in Fig. 10(a) using a fixed step size approach with $\beta = 1$ and Smith prediction with a delay of one. Clearly decision feedback based control struggles to cope with the rapidly changing received signal.

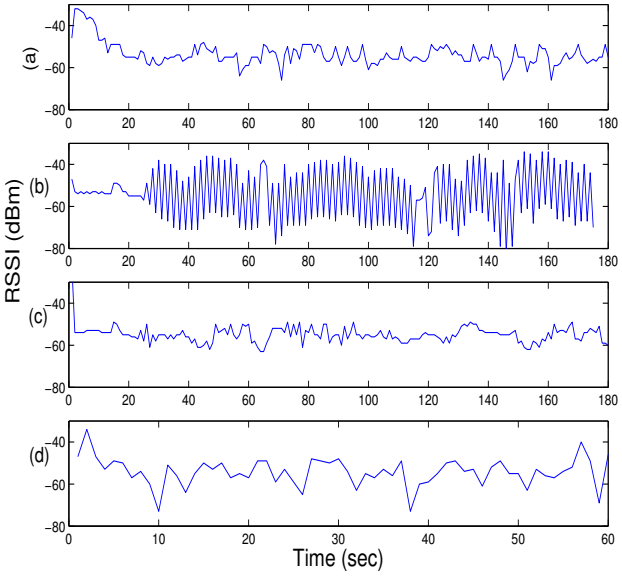

Fig. 10 Mobile Node Power Control

Table 2
Reference Node Power Control Performance. CHARACTERISTICS: σ_e - Standard Deviation (dBm), P_o - Outage Probability (%)

	Fixed Step $\beta = 1$	**Fixed Step** $\beta = 2$	**Fixed Step** $\beta = 1$ **Smith Delay = 1**	**Fixed Step** $\beta = 1$ **Smith Delay = 2**	**Adaptive Forgetting Factor = 0.95**
σ_e	4.57	4.8	2.63	3.92	1.812
P_o	22.4	26.3	14.7	25.69	14.1

	Information $\beta = 0.35$	**Information** $\beta = 0.35$ **Smith Delay = 1**
σ_e	1.62	1.43
P_o	11.88	5.696

Adaptive step size power control again using a forgetting factor of 0.95 is in fact close to unstable in this experiment which may be explained by the inability of the controller to compensate for time delay (see Fig. 10(b)). While Smith prediction was a useful solution to this problem for the reference node case where the delay is constant significant variability will now exist on the delay parameter for the mobile node rendering this approach untenable.

The most satisfactory response is now obtained using information feedback or equation (19), with $\beta = 0.35$ and shown in Fig. 10(c). It is important to note here the speed at which the mobile node is travelling, (in this case the mobile node speed is $0.01m/sec$). As a result multipath fading is not as pronounced as it would be for an agent moving with greater velocity. To characterise this effect, the same experiment is repeated with the mobile node moving at $0.05m/sec$. The results depicted in Fig. 10(d) show that the magnitude of the multipath effects is much more significant in this latter scenario. Note the characteristic deep fades that are far more pronounced at the receiver. The results clearly show that by employing power control floor levels in RSSI can be guaranteed thereby improving PER performance despite a rapidly varying and unpredictable wireless channel, made all the more so by the introduction of mobility in the network.

3.4.4 Power Efficiency

To measure the power efficiency for the respective algorithms, the power efficiency for any one controller configuration is defined as the average power consumed by all motes operating using a particular power control algorithm for the duration of an experiment. For example 100% efficiency in this context would imply that all nodes are transmitting using their minimum output power setting and vice versa. Fig. 11 plots the percentage power efficiency for each of the reference node control configurations. In Fig. 11(a) 1 relates to fixed step power control with $\beta = 1$ or Fig. 8, 2 relates to fixed step with $\beta = 2$ or Fig. 9(a), 3 relates to fixed step with $\beta = 1$ and Smith prediction roundtrip delay = 1 or Fig. 9(b), 4 relates to fixed step with $\beta = 2$ and Smith prediction roundtrip delay = 1 or Fig. 9(c), 5 relates to adaptive control with forgetting factor = 0.95 or Fig. 9(d), 6 relates to information feedback with $\beta = 0.35$ or Fig. 9(e) and 7 relates to Information feedback $\beta = 0.35$ and Smith prediction roundtrip delay =1 or Fig. 9(f). In Fig. 11(b) 1 relates to fixed step with $\beta = 1$ or Fig. 10(a), 2 relates to adaptive control with forgetting factor = 0.95 or Fig. 10(b), 3 relates to information feedback with $\beta = 0.35$ or Fig. 10(c) and 4 relates to Information feedback with $\beta = 0.35$ with speed increased by a factor of 4 or Fig. 10(d).

It is noticeable that the mobile node power control algorithms have lower percentage power efficiency. This might seem strange, but if the path along which the mobile node moves during localization is examined it is clear that the distance from the base station is never as large as the distance to the base station for reference nodes 7,8 and 9 and for much of the experiment reference nodes 4,5 and 6 (see Fig. 5). Therefore it can be expected that decreased power efficiency will be observed for the reference nodes when averaged over all nine nodes.

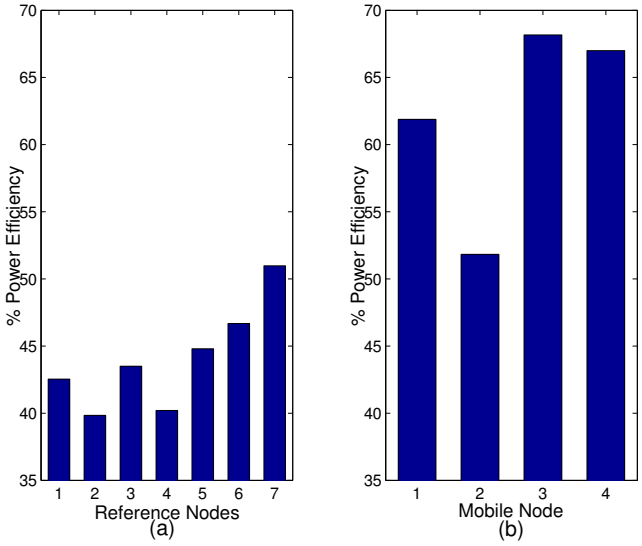

Fig. 11 Power efficiency for each controller configuration where (a) is power efficiency for each of the reference node control configurations and (b) is power efficiency for each of the mobile node power control configurations.

4 CONCLUSIONS

In this work a hybrid localisation and transceiver output power control methodology was proposed and practically validated in a quality of service and power aware wireless sensor network. A systems theoretic solution was presented where firstly a radio frequency based deterministic localisation algorithm was outlined that combined a number of existing strategies into a hybrid multilateration technique using least square estimation. Filtering the received signal strength measurement over time was shown to remove multipath effects which resulted in improved positioning accuracy.

A number of transceiver output power control algorithms were outlined to operate in parallel with the localisation al-

Table 3
Mobile Node Power Control Performance. CHARACTERISTICS: σ_e - Standard Deviation (dBm), P_o - Outage Probability (%)

	Fixed Step $\beta = 1$	**Adaptive Forgetting Factor = 0.95**	**Information** $\beta = 0.35$	**Information** $\beta = 0.35$ **Speed increased to** $0.05m/sec$
σ_e	11.45	16.83	6.61	12.78
P_o	18.77	41.88	14.2	21.3

gorithm. The goal was to alleviate the near-far effect and to limit the negative impact of attenuation, interference and noise. Power control was applied to the uplink between the reference nodes and the base station. A number of algorithms were experimented with and the information feedback approach with Smith prediction proved to be the most effective. This highlighted the advantage associated with using additional feedback bandwidth, where available, and also the need for effective time delay compensation. Transceiver output power control was also implemented on the uplink between the mobile node and the base station. Multipath fading was of primary concern in this instance along with a varying roundtrip delay and information feedback based control proved to be more optimal when compared with other examined approaches.

Finally an adaptive time synchronised approach was employed to ensure the positioning technique operated effectively despite dataloss and a varying transceiver output power from the mobile agent due to power control.

The proposed hybrid methodology was practically tested using an extensive fully scalable and repeatable 802.15.4 compliant experimental testbed. The implementation was framed in an experimental procedure designed to track a moving object in a realistic indoor search and rescue environment.

References

[1] H. Karl and A. Willig. *Protocols and Architectures for Wireless Sensor Networks*. John Wiley and Sons, 2005

[2] E. Cayirci1 and T. Coplu. SENDROM: Sensor networks for disaster relief operations management. *Journal on Wireless Networks*, Vol. 13, No. 3, Pages 409-423, 2007.

[3] U. C. Guard, Navstar GPS User Equipment Introduction (Public Release Version), *Technical Report*, 1996.

[4] S. Pandey and P. Agrawal. A Survey on Localization Techniques for Wireless Networks, *Journal of the Chinese Institute of Engineers*, Vol. 29, No. 7, 2006.

[5] IET Engineering and Technology Magazine. *Rescue robots hit comms snag*, April 2007.

[6] S. Koskie and Z. Gajic. Signal-To-Interference-Based Power Control for Wireless Networks: A Survey, 1992–2005. *Dynamics of Continuous, Discrete and Impulsive Systems B: Applications and Algorithms*, Vol. 13, No. 2, pp. 187220, 2006.

[7] M. J. Walsh, S. M. M. Alavi and M. J. Hayes. On the effect of communication constraints on robust performance for a practical 802.15.4 Wireless Sensor Network Benchmark problem. *In Proc. of the 47th IEEE Conference on Decision and Control Cancun,* Mexico, Dec. 9-11, 2008

[8] B. Zurita Ares, C. Fischione, A. Speranzon, and K. H. Johansson. On power control for wireless sensor networks: system model, middleware component and experimental evaluation. *European Control Conference*, Kos, Greece, 2007.

[9] Yuan-Ho Chen Bore-Kuen Lee and Bor-Sen Chen, Robust Hinf Power Control for CDMA Cellular Communication Systems, *IEEE Transactions on Signal Processing*, 2006, (54)(10): 3947–3956.

[10] N. Patwari and A.O. Hero III. Using proximity and quantized rss for sensor localization in wireless networks. *International Workshop on Wireless Sensor Networks and Applications*, San Diego, Ca, September 2003.

[11] P. Bahl and V. N. Padmanabhan. RADAR: An In-Building RF-Based User Location and Tracking System. *In Proceedings of the IEEE INFOCOM*, Tel Aviv, Israel, March, 2000.

[12] J. Hightower, G. Boriello and R. Want. SpotON: An indoor 3D Location Sensing Technology Based on RF Signal Strength, *University of Washington CSE Report 2000-02-02*, February 2000.

[13] D. Ganesan, B. Krishnamachari, A. Woo, D. Culler, D. Estrin and S. Wicker. Complex Behavior at Scale: An Experimental Study of Low-Power Wireless Sensor Networks, *Technical Report UCLA/CSD-TR 02-0013*, 2002.

[14] T. He, C. Huang, B.M. Blum, J.A. Stankovic, and T. Abdelzaher. Range free localization schemes for large scale sensor networks. *MobiCom*, San Diego, California, USA, September 2003.

[15] K. Yedavalli, B. Krishnamachari, S. Ravula, and B. Srinivasan. Ecolocation: a sequence based technique for rf localization in wireless sensor networks. *Fourth International Symposium on Information Processing in Sensor Networks*, Los Angeles, California, USA, 2005.

[16] S. Feldmann, K. Kyamakya, A. Zapater, and Z. Lue. An indoor bluetooth-based positioning system: concept, implementation and experimental evaluation. *International Conference on Wireless Networks*, Las Vegas, USA, June 2003.

[17] B. Zurita Ares, C. Fischione, A. Speranzon, and K. H. Johansson, On power control for wireless sensor networks: system model, middleware component and experimental evaluation, *European Control Conference*, Kos, Greece, 2007.

[18] A. Goldsmith, *Wireless communications*, Cambridge University Press, 2006.

[19] IEEE Standard. *Wireless lan medium access control (mac) and physical layer (phy) specifications for lowrate wireless personal area networks (lr-wpans)*. IEEE Std 802.15.4, 2006.

[20] F. Gunnarsson, F. Gustafsson, and J. Blom. Pole placement design of power control algorithms. *In Proc. IEEE Vehicular Technology Conference*, Houston, TX, USA, 1999.

[21] A. Salmasi and S. Gilhousen. On the system design aspects of code division multiple access (cdma) applied to digital cellular and personal communications networks. *In Proc. IEEE Vehicular Technology Conference*, New York, NY, USA, May 1991.

[22] K. Astrom and B. Wittenmark. *Computer Controlled Systems Theory and Design.* Prentice-Hall, Englewood Cliffs, NJ, USA, 3rd edition, 1997.

[23] RoboRescue, Available: http://www.rescuesystem.org/robocuprescue, [Accessed January 10, 2009].

[24] J. Polastre, R. Szewczyk, and D. Culler. Telos: enabling ultra-low power wireless research. *Proceedings of the 4th international symposium on Information processing in sensor networks*, Los Angeles, California, USA, 2005.

[25] MIABOT Pro fully autonomous miniature mobile robot, Available: http://www.merlinrobotics.co.uk/merlinrobotics/, [Accessed January 14, 2009].

[26] F. Gunnarsson and F. Gustafsson. Power control in wireless communications networks - from a control theory perspective. *IFAC World Congress*, Barcelona, Spain, 2002.

Michael J. Walsh received a first class honours Bachelor of Engineering Degree in Electronic Engineering from the University of Limerick in 2005. He subsequently applied for and was awarded a PhD scholarship sponsored by the Embark Initiative's Postgraduate Research Scheme under the Irish Council for Science, Engineering and Technology (IRCSET). He completed his PhD, entitled "An Anti-Windup Approach to Reliable Communication and Resource Management in Wireless Sensor Networks", as a member of the Wireless Access Research Centre in the Electronic and Computer Engineering Department at the University of Limerick in 2009. Following completion of his PhD, Michael joined the Tyndall National Institute in Cork, where he is currently a Post-Doctoral Researcher funded by the Clarity Centre for Sensor Web Technologies. His research interests are presently centred on the development of wearable body area networks and more specifically the design and practical evaluation of new miniaturised heterogeneous wearable technologies. He is also concerned with protocol development for wireless body area networks, where his goal is to apply systems science and optimisation techniques in the wireless ambient healthcare environment. E-mail: michael.walsh@tyndall.ie.

Anthony Fee received a 1st class Bachelor of Engineering Degree from the Electronic and Computer Engineering Deparment in the University of Limerick in 2005. He is currently a PhD canditate in the Wireless Access Research group, University of Limerick. His primary research interests include Intelligent Vehicle Systems, Robotics and Sensor fusion. E-mail: anthony.fee@ul.ie.

John Barton received his M Eng Sc degree from UCC in 2006. He joined the Interconnection and Packaging Group of the National Microelectronics Research Centre (now Tyndall National Institute) as a Research Engineer in 1993. Currently in the Wireless Sensor Networks team where his recent research interests include ambient systems research, wearable computing and deployment of wireless sensor networks for personalised health applications. As PI on the Enterprise Ireland funded D-Systems project John has been the leader of the development of the Tyndall Wireless Sensor Mote platform. He has authored or co-authored over 90 peer reviewed papers. E-mail: john.barton@tyndall.ie.

Brendan O'Flynn received his BE Hons from University College Cork in 1993, and his M Eng Sc degree from University College Cork, National Microelectronics Research Centre in 1995. Brendan is a senior staff researcher at the Tyndall national Institute and is Research Activity leader for the Wireless Sensor Network (WSN) group. As such he has been responsible for directing the research activities of the group in a variety of industry funded, nationally funded and European projects. He has been involved in the development of the AES Intern program, and conducting research into miniaturised wireless sensor systems as well as the supervision activities associated with postgraduate students PHD and Masters Level. His research interests include low power microelectronic design, RF system design System integration of miniaturised sensing systems and embedded system design on resource constrained platforms. Brendan was one of the founders of Inpact Microelectronics Ireland Ltd. and has significant expertise in the commercialisation of technology. Inpact (a spin off from the National Microelectronics Research Centre (NMRC)) specialised in the development of System in a Package (SiP) solutions for customers. Inpact offered a complete solution to customers enabling the development of a product concept through to volume product supply; specialising in radio frequency (RF) system development and product miniaturisation. E-mail: brendan.oflynn@tyndall.ie.

Martin J. Hayes has lectured at the University of Limerick since 1997, is currently course leader for the BSc in Electronics programme, and is a Researcher in the Wireless Access Research Centre. He teaches undergraduate and postgraduate courses in Electrical Science, Automatic Control, Computer Controlled Systems and the control of Non-Linear systems. His research interests lie in the area of Systems Theory in general and in particular on the intelligent use of system resources within biomedical or safety critical wireless systems that are subjected to channel and/or performance uncertainties. He is also interested in how the dynamic delivery of information to handheld devices at tourist attractions can add value to the visitor experience. . E-mail: martin.j.hayes@ul.ie.

Cian O'Mathuna is head of Tyndall National Institutes Microsystems Centre. His research interests include microelectronics integration for ambient electronic systems, biomedical microsystems, and energy processing for information and communications technologies. He received his PhD in microelectronics from University College Cork. Hes a member of the IEEE. E-mail: cian.omathuna@tyndall.ie.